

FERROFLUID-LUBRICATED SECANT-SHAPED SQUEEZE-FILM BEARING
WITH ANISOTROPIC PERMEABILITY, SLIP-VELOCITY, MATERIAL
PARAMETER AND ROTATIONAL INERTIA

RAJESH C. SHAH^a and M. V. BHAT^b

^a*Department of Mathematics, Government Engineering College, Polytechnic Campus,
Sector - 26, Gandhinagar - 382 044, Gujarat State, India*

^b*E-202, Riddhi Complex, Near Jodhpur Village, Ahmedabad - 380 015, Gujarat State,
India*

Received 19 September 2006; Accepted 5 December 2007

Online 8 February 2008

We present a theoretical study of the effect of anisotropic permeability and slip velocity on the action of the squeeze film formed when a secant-shaped circular upper plate with a porous facing approaches an impermeable and flat circular lower plate, considering also rotation of the plates. Expressions for the dimensionless pressure, load capacity and the response time are given by a differential equation. Computed values of dimensionless load capacity and response time are displayed in tabular form. It has been found that they decrease with increasing values of radial permeability, slip parameter and rotational inertia. However, they increase with increasing values of axial permeability and material constant of the Jenkins model. They have also been found to increase when the speed of the lower plate is higher than that of the upper plate.

PACS numbers: 81.40.Pq, 46.55.+d

UDC 531.44, 532.516

Keywords: ferrofluid, lubrication, squeeze film, anisotropic permeability, slip, rotational inertia, Jenkins model, Neuringer-Rosensweig model

1. Introduction

Sparrow et al. [1] and Prakash et al. [2] studied the effect of velocity slip on the porous-walled squeeze films. Kulkarni et al. [3] obtained a general equation to study the lubrication of anisotropic porous bearings considering the slip velocity at the porous-film interface.

Ferrofluid was used as a lubricant by Shah et al. [4] and Patel et al. [5] to

study the squeeze film behaviour in curved rotating porous circular plates and the squeeze film between two secant-shaped circular plates respectively, using Neuringer-Rosensweig model. Ram and Verma [6] analysed a porous inclined slider bearing using Jenkins model for the lubricant flow. Later on Shah et al. [7–9] studied parallel plate slider bearing, exponential shape squeeze film bearing and journal bearing using the flow model given by Jenkins with a different view points. All the above investigators used an oblique external field, the values of the bearing characteristics being not affected by the obliqueness of the field.

In this paper our aim is to consider a squeeze film formed between two circular plates, the upper one being secant-shaped with a porous facing and to study the effects of anisotropic permeability, slip velocity and rotation of both the plates on it with a ferrofluid lubricant which flows as per Jenkins flow behaviour which takes care of material constant. A secant-shaped upper plate is chosen because it wins over the flat plate and is a useful introduction to the parabolic or journal shape [10].

2. Analysis

The bearing, shown in Fig. 1, consists of two circular plates, each of radius a . The upper plate is secant-shaped and has a porous facing of thickness H_0 which is backed by a solid wall. It moves normally towards the impermeable and flat lower plate with a uniform velocity

$$\dot{h}_0 = \frac{dh_0}{dt},$$

where h_0 is the central film thickness and t is time. The film thickness h is given by

$$h = h_0 \sec(\beta r^2), \quad 0 \leq r \leq a, \quad (1)$$

where β is a factor indicating the curvature of the upper plate and r is the radial coordinate. The upper and lower plates rotate with angular velocities Ω_u and Ω_l ,

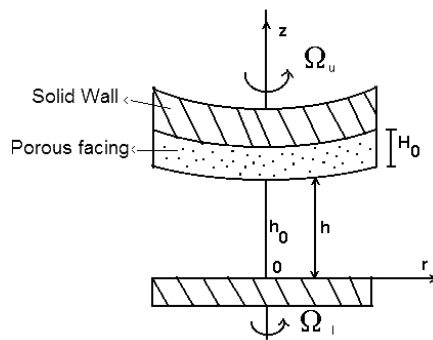


Fig. 1. Configuration of the problem.

respectively. Assuming axisymmetric flow of the ferrofluid between the plates under an oblique magnetic field whose magnitude H is given by

$$H^2 = Kr^2(a - r)/a, \quad (2)$$

where K is chosen to suit the dimensions of both sides.

As shown in the Appendix, one obtains the Reynolds type equation in this case as

$$\begin{aligned} & \frac{1}{r} \frac{d}{dr} \left[\left\{ 12\phi_r H_0 + \frac{h^3(4 + sh) - 3s\rho\alpha^2\bar{\mu}\phi_z h^2 H/\eta}{(1 + sh)[1 - \rho\alpha^2\bar{\mu}H/(2\eta)]} + \frac{6\rho\alpha^2\bar{\mu}(\phi_r - \phi_z)H_0 H}{\eta[1 - \rho\alpha^2\bar{\mu}H/(2\eta)]} \right\} \right. \\ & \quad \left. \times r \frac{d}{dr} \left(p - \frac{1}{2}\mu_0\bar{\mu}H^2 \right) \right] \\ & = 12\eta\dot{h}_0 + 24\rho\Omega_u^2\phi_r H_0 + 6\rho\alpha^2\bar{\mu}(\phi_r - \phi_z) \frac{H_0}{\eta r} \frac{d}{dr} \left(\frac{\rho r^2 \Omega_u^2 H}{1 - \rho\alpha^2\bar{\mu}H/(2\eta)} \right) \\ & \quad - s\rho^2\alpha^2\bar{\mu} \frac{\phi_z(3\Omega_r^2 + 8\Omega_l\Omega_r + 6\Omega_l^2)}{2\eta r} \frac{d}{dr} \left\{ \frac{r^2 h^2 H}{(1 + sh)[1 - \rho\alpha^2\bar{\mu}H/(2\eta)]} \right\} \\ & \quad + \frac{\rho}{r} \frac{d}{dr} \left[\frac{r^2 h^3 \{0.3(6 + sh)\Omega_r^2 + (5 + sh)\Omega_r\Omega_l + (4 + sh)\Omega_l^2\}}{(1 + sh)[1 - \rho\alpha^2\bar{\mu}H/(2\eta)]} \right]. \end{aligned} \quad (3)$$

Using Eqs. (1)–(2) and the dimensionless quantities

$$\begin{aligned} R &= \frac{r}{a}, & \bar{h} &= \frac{h}{h_0}, & \Psi_r &= \frac{\phi_r H_0}{h_0^3}, & \Psi_z &= \frac{\phi_z H_0}{h_0^3}, \\ \gamma^* &= \frac{6\phi_z}{h_0^2}, & \bar{s} &= sh_0, & \delta &= \frac{\rho\alpha^2\bar{\mu}\sqrt{K}a}{2\eta}, & \mu^* &= -\frac{K\mu_0\bar{\mu}h_0^3}{\eta\dot{h}_0}, \\ \bar{p} &= -\frac{h_0^3 p}{\eta a^2 \dot{h}_0}, & S &= -\frac{\rho\Omega_u^2 h_0^3}{\eta\dot{h}_0}, & \Omega_f &= \frac{\Omega_l}{\Omega_u}, & \bar{\beta} &= \beta a^2 \end{aligned} \quad (4)$$

reduces Eq. (3) to

$$\frac{1}{R} \frac{d}{dR} \left[GR \frac{d}{dR} \left\{ \bar{p} - \frac{1}{2}\mu^* R^2(1 - R) \right\} \right] = \frac{1}{R} \frac{d}{dR} (RF), \quad (5)$$

where

$$F = -6R + 12\Psi_r SR + \frac{12\delta(\Psi_r - \Psi_z)SR^2\sqrt{1 - R}}{1 - \delta R\sqrt{1 - R}} \quad (6)$$

$$-SR\bar{h}^2 \frac{5\bar{s}\delta\gamma^*(3+2\Omega_f+\Omega_f^2)R\sqrt{1-R}-3\bar{h}\{3\bar{s}\bar{h}+18+(4\bar{s}\bar{h}+14)\Omega_f+(3\bar{s}\bar{h}+8)\Omega_f^2\}}{30(\bar{s}\bar{h}+1)(1-\delta R\sqrt{1-R})},$$

$$G = \frac{12(\Psi_r - \delta\Psi_z R\sqrt{1-R})(1 + \bar{s}\bar{h}) + \bar{h}^3(4 + \bar{s}\bar{h}) - \delta\gamma^*\bar{s}\bar{h}^2 R\sqrt{1-R}}{(1 + \bar{s}\bar{h})(1 - \delta R\sqrt{1-R})}. \quad (7)$$

Note that $F = F(\Psi_r, \Psi_z, S, \bar{s}, \gamma^*, \bar{h}, \Omega_f, \delta, R)$, $G = G(\Psi_r, \Psi_z, S, \bar{s}, \gamma^*, \bar{h}, \Omega_f, \delta, R)$ and $\bar{h} = \sec(\bar{\beta}R^2)$.

3. Solutions

Solving Eq. (5) under the boundary conditions

$$\bar{p}(1) = 0, \quad \frac{d\bar{p}}{dR} = 0 \quad \text{when} \quad R = 0, \quad (8)$$

yields

$$\bar{p} = \frac{1}{2}\mu^*R^2(1-R) + \int_1^R \frac{F}{G} dR. \quad (9)$$

The load capacity W of the bearing is given in dimensionless form as

$$\bar{W} = -\frac{h_0^3 W}{2\pi\eta a^4 h_0} = \frac{\mu^*}{40} - \frac{1}{2} \int_0^1 \frac{R^2 F}{G} dR. \quad (10)$$

The response time t to reach a film thickness h_0 starting with an initial value h_1 is given in dimensionless form by the equation

$$\frac{d\bar{t}}{d\bar{h}_0} = \frac{3 \int_0^1 (R^3/G^*) dR}{-(1/2\pi) + \mu_1^*/40 - (1/2) \int_0^1 (R^2 F^*/G^*) dR}, \quad (11)$$

where

$$\bar{h}_0 = \frac{h_0}{h_1}, \quad \mu_1^* = \frac{K\mu_0\bar{\mu}a^4}{W}, \quad \Psi_r^* = \frac{\phi_r H_0}{h_1^3}, \quad \Psi_z^* = \frac{\phi_z H_0}{h_1^3}, \quad (12)$$

$$\gamma_1^* = \frac{6\phi_z}{h_1^2}, \quad \bar{t} = \frac{h_1^2 W t}{\eta a^4}, \quad s^* = s h_1, \quad S_1 = \frac{\rho a^4 \Omega_u^2}{W},$$

and

$$F^* = 6R + F(\Psi_r^*, \Psi_z^*, S_1, s^*, \gamma_1^*, \bar{h}_0\bar{h}, \Omega_f, \delta, R), \quad (13)$$

$$G^* = G(\Psi_r^*, \Psi_z^*, S_1, s^*, \gamma_1^*, \bar{h}_0\bar{h}, \Omega_f, \delta, R). \quad (14)$$

4. Results and discussion

Eqs. (9)–(11) give the dimensionless pressure \bar{p} , load capacity \bar{W} and response time \bar{t} of the squeeze film. We computed the values of \bar{W} and \bar{t} taking the modified representative values of parameters from Ref. [4]: $a = 0.05$ m, $h_0 = 2.5 \times 10^{-5}$ m, $\eta_r = 0.25$, $W = 50$ kg m s⁻², $\eta = 2 \times 10^{-3}$ kg m⁻¹ s⁻¹, $\bar{\mu} = 0.05$, $\mu_0 = 4\pi \times 10^{-7}$ kg m s⁻² A⁻², $\rho = 800$ kg m⁻³, $\max(H) = 1.9 \times 10^5$ A m⁻¹, $S = 0.25$ and $S_1 = 0.01$ when $\Omega_u = 10$ rad/s.

The computed the values of \bar{W} and \bar{t} are displayed in Tables 1–9.

Table 1 shows that \bar{W} decreases with increasing values of radial permeability parameter ϕ_r/h_0^2 and increases with increasing values of axial permeability parameter ϕ_z/h_0^2 . The downward diagonal values are the values of \bar{W} in the isotropic case, $\phi_r = \phi_z$, which decrease with increasing values of the permeability parameter. However, \bar{W} increases for reducing ϕ_r/h_0^2 and increasing ϕ_z/h_0^2 . While the rotational parameter S increases, \bar{W} reduces when ϕ_z/h_0^2 is less than 10^{-4} and it increases otherwise as shown in Table 2. At $\delta = 0$, \bar{W} reduces as S increases. For

TABLE. 1. Values of \bar{W} for different values of ϕ_r/h_0^2 and ϕ_z/h_0^2 .

ϕ_z/h_0^2	ϕ_r/h_0^2				
	10^{-7}	10^{-6}	10^{-5}	10^{-4}	10^{-3}
10^{-7}	2.8779	1.212	1.046	1.0247	0.9769
10^{-6}	19.5336	2.878	1.212	1.0412	0.9784
10^{-5}	186.123	19.54	2.877	1.2064	0.9936
10^{-4}	1855.17	186.49	19.56	2.8613	1.1456
10^{-3}	18867.6	1887.8	189.6	19.727	2.6920

$$\delta = 0.5, \mu^* = 19.6, S = 0.25, \Omega_f = 1.0, H_0/h_0 = 10, \bar{\beta} = 0.4.$$

TABLE. 2. Values of \bar{W} for different values of ϕ_z/h_0^2 and S .

S	ϕ_z/h_0^2				
	10^{-7}	10^{-6}	10^{-5}	10^{-4}	10^{-3}
0.0625	1.0002	1.0006	1.0045	1.0430	1.4348
0.25	0.9769	0.9784	0.9936	1.1456	2.6920
1.00	0.8837	0.8897	0.9502	1.5561	7.7206
2.25	0.7283	0.7419	0.8779	2.2402	16.102
4.00	0.5107	0.5349	0.7766	3.1979	27.835

$$\phi_r/h_0^2 = 10^{-3}, \delta = 0.5, \mu^* = 19.6, \Omega_f = 1.0, H_0/h_0 = 10, \bar{\beta} = 0.4.$$

δ values upto 1.5, \bar{W} increases for increasing S as shown in Table 3. In fact \bar{W} attains a maximum value when δ is nearly unity. On the other hand, Table 4 shows that \bar{W} attains a minimum when the plates rotate in opposite directions with the same speed and that \bar{W} can be increased by choosing the speed of the lower plate large compared to that of the upper plate.

Table 5 shows that \bar{t} slowly decreases when ϕ_r/h_0^2 increases or in the isotropic case ($\phi_r = \phi_z$). But \bar{t} increases with increasing values of ϕ_z/h_0^2 . Table 6 shows that \bar{t} decreases when S_1 increases. It can be seen from Table 7 that \bar{t} generally decreases with increasing values of the material constant parameter δ .

Table 8 shows that \bar{t} attains a maximum when the plates rotate in opposite directions with the same speed. It can be seen from Table 9 that values of \bar{W} and \bar{t} are larger in the case of flat upper plate ($\bar{\beta} = 0$) than those in the case of secant-shaped upper plate as would be expected.

TABLE. 3. Values of \bar{W} for different values of δ and S .

S	δ			
	0.0	0.5	1.0	1.5
0.0625	1.1474	1.513	1.5470	1.3626
0.25	1.1240	2.877	3.3031	2.8562
1.00	1.0303	8.333	10.328	8.8302
2.25	0.8740	17.427	22.035	18.787
4.00	0.6553	30.158	38.425	32.727

$$\phi_r/h_0^2 = \phi_z/h_0^2 = 10^{-5}, \mu^* = 19.6, \Omega_f = 1.0, H_0/h_0 = 10, \bar{\beta} = 0.4.$$

TABLE. 4. Values of \bar{W} for different values of Ω_f and S .

S	Ω_f						
	-5	-2	-1	0	1	2	5
0.0625	2.4007	1.2842	1.2111	1.2874	1.5132	1.8884	3.9111
0.25	6.4272	1.9616	1.6689	1.9741	2.8772	4.3782	12.469
1.00	22.534	4.6709	3.5000	4.7209	8.3334	14.338	46.700
2.25	49.377	9.1864	6.5520	9.2989	17.427	30.937	103.75
4.00	86.958	15.508	10.825	15.708	30.158	54.175	183.63

$$\phi_r/h_0^2 = \phi_z/h_0^2 = 10^{-5}, \mu^* = 19.6, \delta = 0.5, H_0/h_0 = 10, \bar{\beta} = 0.4.$$

TABLE. 5. Values of \bar{t} for different values of ϕ_r/h_0^2 and ϕ_z/h_0^2 .

ϕ_z/h_0^2	ϕ_r/h_0^2				
	10^{-7}	10^{-6}	10^{-5}	10^{-4}	10^{-3}
10^{-7}	1.1363	1.1364	1.1356	1.1224	0.9929
10^{-6}	1.1363	1.1364	1.1356	1.1224	0.9929
10^{-5}	1.1366	1.1367	1.1359	1.1227	0.9931
10^{-4}	1.1390	1.1391	1.1383	1.1250	0.9949
10^{-3}	1.1640	1.1641	1.1632	1.1493	1.0135

$\delta = 0.5, \mu^* = 19.6, S = 0.25, \Omega_f = 1.0, H_0/h_0 = 10, \bar{\beta} = 0.4, \bar{h}_0 = 0.8.$

TABLE. 6. Values of \bar{t} for different values of ϕ_z/h_0^2 and S_1 .

S_1	ϕ_r/h_0^2				
	10^{-7}	10^{-6}	10^{-5}	10^{-4}	10^{-3}
0.0025	0.9995	0.9995	0.9997	1.0015	1.0203
0.01	0.9929	0.9929	0.9931	0.9949	1.0135
0.04	0.9671	0.9671	0.9673	0.9690	0.9872
0.09	0.9270	0.9270	0.9272	0.9289	0.9463
0.16	0.8761	0.8761	0.8763	0.8779	0.9844

$\phi_r/h_0^2 = 10^{-3}, \delta = 0.5, \mu_1^* = 0.785, \Omega_f = 1.0, H_0/h_0 = 10, \bar{\beta} = 0.4, \bar{h}_0 = 0.8.$

TABLE. 7. Values of \bar{t} for different values of δ and S_1 .

S_1	δ			
	0.0	0.5	1.0	1.5
0.0025	1.3381	1.1435	0.9488	0.7540
0.01	1.3292	1.1359	0.9425	0.7490
0.04	1.2946	1.1064	0.9180	0.7295
0.09	1.2410	1.0605	0.8799	0.6992
0.16	1.1729	1.0023	0.8317	0.6609

$\phi_r/h_0^2 = \phi_z/h_0^2 = 10^{-5}, \mu_1^* = 0.785, \Omega_f = 1.0, H_0/h_0 = 10, \bar{\beta} = 0.4, \bar{h}_0 = 0.8.$

TABLE. 8. Values of \bar{t} for different values of Ω_f and S_1 .

S_1	Ω_f						
	-5	-2	-1	0	1	2	5
0.0025	1.1314	1.1443	1.1455	1.1453	1.1435	1.1402	1.1214
0.01	1.0894	1.1389	1.1440	1.1430	1.1359	1.1229	1.0536
0.04	0.9489	1.1180	1.1379	1.1338	1.1064	1.0588	0.8483
0.09	0.7809	1.0847	1.1278	1.1189	1.0605	0.9668	0.6403
0.16	0.6258	1.0414	1.1140	1.0987	1.0023	0.8619	0.4767

$$\phi_r/h_0^2 = \phi_z/h_0^2 = 10^{-5}, \mu_1^* = 0.785, \delta = 0.5, H_0/h_0 = 10, \bar{\beta} = 0.4, \bar{h}_0 = 0.8.$$

TABLE. 9. Values of \bar{W} and \bar{t} for different values of $\bar{\beta}$ and δ .

δ	\bar{W}		\bar{t}	
	$\bar{\beta}$			
	0	0.4	0	0.4
0.0	1.1148	1.0303	1.4591	1.2947
0.5	8.4077	8.3334	1.2520	1.1064
1.0	10.392	10.328	1.0447	0.9180
1.5	8.8853	8.8302	0.8372	0.7295

$$\phi_r/h_0^2 = \phi_z/h_0^2 = 10^{-5}, \mu^* = 19.6, S = 1.0, S_1 = 0.04, \Omega_f = 1.0, H_0/h_0 = 10, \mu_1^* = 0.785, \bar{h}_0 = 0.8.$$

As the slip parameter $1/\bar{s}$ is proportional to

$$\sqrt{\phi_r}/h_0,$$

\bar{W} and \bar{t} decrease when $1/\bar{s}$ increases, as seen from Table 1 and Table 5.

Thus anisotropic permeability can be used to counter the effect of slip velocity.

The results for the corresponding case of the lubricant flow following Neuringer-Rosenzweig model can be deduced from the present case by setting $\delta = 0$.

dovde

5. Conclusions

In the designing a porous secant-shaped squeeze film bearing the decrease in the values of bearing characteristics owing to slip velocity can be countered by suitably

choosing anisotropic permeability of the porous matrix. However, the values of bearing characteristics are always less than the corresponding parallel-plate squeeze film bearing.

The results obtained above are more practical over the other models due to the consideration of the effect of material constant.

Appendix

The governing equations for the present case are [2, 6]

$$\frac{\partial^2 u}{\partial z^2} = \frac{1}{\eta[1 - \rho\alpha^2\bar{\mu}H/(2\eta)]} \left[\frac{d}{dr} \left(p - \frac{1}{2}\mu_0\bar{\mu}H^2 \right) - \rho r \left(\frac{z}{h}\Omega_r + \Omega_l \right)^2 \right], \quad (A.1)$$

where u is the radial velocity of the film fluid, p is the film pressure, η is the fluid viscosity, ρ is the fluid density, α^2 is the material constant, $\bar{\mu}$ is the magnetic susceptibility, μ_0 is the permeability of free space, z is the axial coordinate and $\Omega_r = \Omega_u - \Omega_l$, and

$$\frac{1}{r} \frac{\partial}{\partial r}(ru) + \frac{\partial w}{\partial z} = 0, \quad (A.2)$$

where w is the axial component of film fluid.

Solving Eq. (A.1) under the slip boundary conditions [1]

$$u = 0 \quad \text{when} \quad z = 0, \quad u = -\frac{1}{s} \frac{\partial u}{\partial z} \quad \text{when} \quad z = h; \quad \frac{1}{s} = \frac{\sqrt{\phi_r \eta_r}}{5}, \quad (A.3)$$

where ϕ_r and η_r are the permeability and porosity of the porous facing in the radial direction and s is the slip coefficient, one obtains

$$u = \frac{z}{2\eta(1 + sh)[1 - \rho\alpha^2\bar{\mu}H/(2\eta)]} \times \left[(hsz - sh^2 + z - 2h) \frac{d}{dr} \left(p - \mu_0\bar{\mu}H^2/2 \right) - \frac{\rho r}{6h^2} \left\{ (z^3 sh - h^4 s + z^3 - 4h^3)\Omega_r^2 + 4h(z^2 sh - sh^3 + z^2 - 3h^2)\Omega_r\Omega_l + 6h^2(zsh - h^2 s + z - 2h)\Omega_l^2 \right\} \right]. \quad (A.4)$$

The radial and axial components \bar{u} , \bar{w} of the velocity of the fluid in the porous matrix are, respectively,

$$\bar{u} = -\frac{\phi_r}{\eta} \left[\frac{\partial}{\partial r} \left(P - \frac{1}{2}\mu_0\bar{\mu}H^2 \right) - \rho\Omega_u^2 r + \frac{\rho\alpha^2\bar{\mu}}{2} \frac{\partial}{\partial z} \left(H \frac{\partial u}{\partial z} \right) \right], \quad (A.5)$$

$$\bar{w} = -\frac{\phi_z}{\eta} \left[\frac{\partial}{\partial z} \left(P - \frac{1}{2}\mu_0\bar{\mu}H^2 \right) - \frac{\rho\alpha^2\bar{\mu}}{2r} \frac{\partial}{\partial r} \left(rH \frac{\partial u}{\partial z} \right) \right], \quad (A.6)$$

where ϕ_z is the permeability of the porous fluid in the axial direction and P is the fluid pressure. The following continuity equation is valid

$$\frac{1}{r} \frac{\partial}{\partial r}(r\bar{u}) + \frac{\partial \bar{w}}{\partial z} = 0. \quad (\text{A.7})$$

Substituting Eqs. (A.5)–(A.6) into Eq. (A.7) and integrating across the porous matrix, we obtain

$$\begin{aligned} \frac{\phi_r H_0}{r} \frac{d}{dr} \left\{ r \frac{d}{dr} \left(p - \frac{1}{2} \mu_0 \bar{\mu} H^2 \right) \right\} - 2\rho \Omega_u^2 \phi_r H_0 - \phi_z \frac{\partial}{\partial z} \left(P - \frac{1}{2} \mu_0 \bar{\mu} H^2 \right) \Big|_{z=h} \\ + \frac{\rho \alpha^2 \bar{\mu}}{2} (\phi_r - \phi_z) \frac{1}{r} \frac{\partial}{\partial r} \left(r H \frac{\partial u}{\partial z} \right) \Big|_{z=h}^{h+H_0} = 0, \end{aligned} \quad (\text{A.8})$$

using Morgan-Cameron approximation to get the first term and the act that the surface $z = h + H_0$ is impermeable.

Using Eq. (A.4), Eq. (A.8) yields

$$\begin{aligned} \frac{\partial}{\partial z} \left(P - \frac{1}{2} \mu_0 \bar{\mu} H^2 \right) \Big|_{z=h} = \frac{\phi_r H_0}{r \phi_z} \frac{d}{dr} \left\{ r \frac{d}{dr} \left(p - \frac{1}{2} \mu_0 \bar{\mu} H^2 \right) \right\} - \frac{2\rho \Omega_u^2 \phi_r H_0}{\phi_z} \\ + \frac{\rho \alpha^2 \bar{\mu}}{2\eta \phi_z} (\phi_r - \phi_z) \frac{H_0}{r} \frac{d}{dr} \left(\frac{rH}{1 - (\rho \alpha^2 \bar{\mu} H)/(2\eta)} \left\{ \frac{d}{dr} \left(p - \frac{1}{2} \mu_0 \bar{\mu} H^2 \right) - \rho r \Omega_u^2 \right\} \right). \end{aligned} \quad (\text{A.9})$$

As the fluid velocity components across the film-porous interface are continuous

$$\begin{aligned} w_{z=h} = \bar{w}_{z=h} = \dot{h}_0 - \frac{\phi_z}{\eta} \left[\frac{\partial}{\partial z} \left(P - \frac{1}{2} \mu_0 \bar{\mu} H^2 \right) \right]_{z=h} - \frac{\phi_z s \rho \alpha^2 \bar{\mu}}{2\eta} \\ \times \frac{1}{r} \frac{d}{dr} \left[\frac{rHh^2}{2\eta(sh+1)(1-\rho\alpha^2\bar{\mu}H/(2\eta))} \left\{ \frac{d}{dr} \left(p - \frac{1}{2} \mu_0 \bar{\mu} H^2 \right) - \frac{\rho r}{6} (3\Omega_r^2 + 8\Omega_l \Omega_r + 6\Omega_l^2) \right\} \right] \end{aligned} \quad (\text{A.10})$$

using Eqs. (A.4) and (A.6).

Integrating Eq. (A.2) across the film thickness and using Eqs. (A.9)–(A.10), one obtains the Reynolds-type equation (3) of the text.

References

- [1] E. M. Sparrow, G. S. Beavers and I. T. Hwang, *Trans. ASME*, F **94** (3) (1972) 260.
- [2] J. Prakash and S. K. Vij, *Wear* **38** (1976) 73.
- [3] S. V. Kulkarni and Vinay Kumar, *J. Inst. Eng. (India) Mech. Eng. Div.* **56** (3) (1975) 110.

- [4] R. C. Shah and M. V. Bhat, *J. Magn. Magn. Mater.* **208** (2000) 115.
- [5] R. M. Patel and G. M. Deheri, *Indian J. Eng. and Mater. Science* **9** (2002) 45.
- [6] Paras Ram and P. D. S. Verma, *Indian J. Pure and Appl. Math.* **30** (12) (1999) 1273.
- [7] R. C. Shah and M. V. Bhat, *Industrial Lubrication and Tribology* **57** (3) (2005) 103.
- [8] R. C. Shah and M. V. Bhat, *Eur. J. Mech. Environmental Eng.* **48** (4) (2003) 261.
- [9] R. C. Shah and M. V. Bhat, *J. Magn. Magn. Mater.* **279** (2-3) (2004) 224.
- [10] A. Cameron and C. M. McEttles, *Basic Lubrication Theory*, Wiley (1981) p. 52.

LEŽAJ SA STISNUTIM SLOJEM FEROFLLUIDA, UZ ANISOTROPNU
PERMEABILNOST, PARAMETAR KLIZNE BRZINE MATERIJALA I
TROMOST VRTNJE

Opisujemo teoriju djelovanja anizotropne permeabilnosti i brzine klizanja na učinak stisnutog sloja koji nastaje kada se gornja ploča sekantnog oblika s poroznom površinom nasloni na nepropusnu i ravnu kružnu donju ploču. Bezdimenzijski tlak, nosivost i vrijeme odziva izražavamo diferencijalnom jednačbom. Izračunate vrijednosti za nosivost i vrijeme odziva prikazujemo u tablicama. Nalazi se da one opadaju pri porastu radijalne permeabilnosti, parametra klizanja i momenta tromosti. Međutim, one se povećavaju pri porastu aksijalne permeabilnosti i konstante materijala prema Jenkinsovom modelu. Također nalazimo da rastu kada je brzina gornje veća od brzine donje ploče.